Stator Core with Slits in Transverse Flux Rotary Machine to Reduce Eddy Current Loss

Ji-Young Lee[1]*, Dae-Hyun Koo[1], Do-Hyun Kang[1], and Jung-Pyo Hong[2]

[1]Korea Electrotechnology Research Institute, Changwon, Gyeongnam 641-120, Korea
[2]Department of Automotive Engineering, Hanyang University, Seoul 133-791, Korea

This paper presents an eddy current loss analysis for a transverse flux rotary machine (TFRM) with laminated stator cores, which consist of inner and outer cores whose laminated directions are perpendicular to each other. Although the TFRM is laminated to reduce eddy current losses, it still exhibits rapidly increasing core losses as the frequency increases. To solve this problem, slits are introduced to the stator outer core. 3-dimensional finite element analysis (3D FEA) based on the T-Ω formulation is used to solve the eddy-current problem for a various numbers of slits in the nonlinear lamination core. The effects of the slits are confirmed using experiment data and 3D FEA results.

Keywords : eddy current, finite element analysis, lamination core, slit

1. Introduction

Many papers have presented eddy current analysis for laminated cores [1-5]. Most of these analysis models are related to large size electric machines such as turbine generators and transformers [1-3], or those for high harmonic applications such as reactors [4, 5]. In those applications, the eddy current loss by the flux, which is perpendicular to the laminated cores, is only a few percentages of the total iron losses. However, the effect cannot be overlooked because of heat problems. Due to this, segmented stator cores with lapping between adjacent layers [1] or slits on the stator teeth and the reactor cores to reduce eddy current losses on each steel sheet [1, 2], [4-6] have been adopted.

In comparison with the above conventional electric machine examples, the transverse flux rotary machine (TFRM), which is presented in this paper, have some similarities and some differences regarding eddy current loss.

One of the main differences is that the TFRM has a lower frequency and smaller volume than conventional electric machines. Its fundamental magnetic frequency is 150 Hz at the rated speed, the output power is under 1 kW, the outer diameter is 206 mm and the axial length is 112 mm. If a general longitudinal flux rotary machine (LFRM), similar to the machines in [1-3], had these characteristics the eddy current loss would not be quite as severe a problem because of the laminated cores. The TFRM in this paper also has laminated stator cores, these consist of inner and outer cores whose laminated directions are perpendicular to each other considering magnetic flux path. However, the TFRM has huge eddy current loss in the stator.

To solve this problem slits are introduced in the stator outer core, and this is similar to the above electric machine examples. Strictly speaking, it is the common knowledge that eddy current loss is reduced because the length of the eddy current path is reduced by the slits. However, the slit shape is different from those used for LFRMs because the conditions causing the eddy currents and the eddy current path are different. The slits of the TFRM entirely separate the stator outer core into several fragments rather than only partially separating the outer core like those in LFRMs, such as the large size turbine generators in [1] or induction motors in [6]. Although several partial slits on a stator core such as those in [7] have been tried, there was not a significant reduction in eddy current loss.

In this paper, the eddy current loss and slit effect on the laminated stator core of the TFRM are investigated using

*Corresponding author: Tel: +82-55-280-1416
Fax: +82-55-280-1490, e-mail: jylee@keri.re.kr

experiment and 3-dimensional finite element analysis (3D FEA). First, the analysis model and method are introduced, and then the measured and calculated results are compared in order to verify the validity of the analysis and show how severe the eddy current loss is. Next, the variation of the losses with the number of slits employed is also investigated using both experiment and 3D FEA based on the T-Ω formulation, where T denotes the electric vector potential representing eddy currents in the conducting regions and Ω denotes the magnetic scalar potential [3, 8, 9].

2. Analysis Model and Method

2.1. Analysis model

Fig. 1 shows the configuration of one phase part in a prototype permanent magnet (PM) TFRM, and this also acts as the analysis model for the 3D FEA. The specifications for analysis are listed in Table 1. The phase windings of this prototype TFRM are arranged in an axial direction (z-direction), and magnetically and mechanically separated from each other [10, 11]. As such, one phase modelling is possible for the electromagnetic field analysis. The PMs on rotor are arranged and magnetized around the circumference, as shown in Fig. 1(a), to concentrate the magnetic flux to the soft magnetic composite (SMC) core.

The stator core is divided into two parts, the inner and outer cores that are laminated perpendicular to each other. The inner and outer cores are laminated in the θ and z directions, respectively, as shown in Fig. 1(b). The outer core is again divided into upper and lower parts, the lower part is shifted by a half pole-pitch with respect to the upper part to make magnetic circuits. A phase current coil is wound around the inner core and between the upper and lower outer cores. When current flows counter-clock-
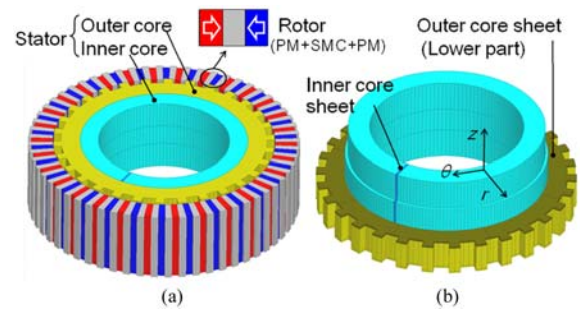

Fig. 1. (Color online) A prototype TFRM. (a) Analysis model, (b) Inner and outer cores.

wise, the magnetic flux flows into the lower part of the outer core and come out from the upper part of the outer core. Between the lower and upper parts of the outer cores, the magnetic flux flows through the inner core. It looks like that both the inner and outer laminations accommodate the flux flows and do not interfere. The lamination is also intended to reduce core losses. As mentioned before, however, the core loss is much more severe than expected, this will be shown in the next section (III).

2.2. Analysis method

Time-harmonic FEA of the 3D electromagnetic field in the prototype TFRM based on the T-Ω formulation was carried out. The FEA was performed with a commercial software package, and the related governing equations are introduced in [9].

Core losses in the lamination core can be divided into four types: eddy current loss caused by the normal component of flux density (so-called 'conducting eddy current loss' in here), eddy current loss caused by the tangential components of flux density, hysteresis loss and excess loss [9]. The three losses, but not the conducting eddy current loss, can be calculated with general formulations consisting of each loss coefficient, frequency, and flux density amplitude. These loss coefficients are not related to the width of the core sheet. So, these three losses are not affected by slits in the core. However the conducting eddy current loss is related to the width of the core sheet because the eddy current path is on the plane of the core sheet. Therefore, the conducting eddy current loss is only dealt with when looking into the effect of the slits.

Since the whole one phase model is used as the analysis region, the boundary condition enclosing the analysis model is Neumann where H is tangential to the boundary and flux cannot cross it. For insulation between the steel sheets and slits, an insulating boundary is used. The condition is the same as Neumann except that the current cannot cross the boundary.

Table 1. Specifications of the Analysis Model

Quantity	Values
Rated speed and its electrical frequency	300 rpm, 150 Hz
No. of serial conductors	90 turns/phase
No. of parallel circuit	2 circuits/phase
No. of rotor pole and stator tooth pairs	30 pairs/phase
No. of phase	2 phases
Rotor/Stator outer diameter	206/145 mm
Axial length	112 mm
Air gap	0.5 mm
Thickness of laminations for stator core	0.5 mm
Material of stator core	Laminated Silicon Steel
Conductivity of stator core	3×10^6 S/m

3. Loss Problem

The stator outer core of the prototype TFRM was made as shown in Fig. 2(a). The average static torques due to magneto motive forces, which are the products of currents by number of turns, were measured for one phase, and compared with the calculated results obtained by FEA as shown in Fig. 3. The results are in good agreement with each other when the rotational speed is zero.

However, when the no-load electro-motive force (EMF) was measured with the rotor rotating, the curve of the EMF with rotation speed was severely nonlinear, as shown in Fig. 4. The EMF values were regulated on the basis of the calculated EMF at 600 Hz as 100%. The error between the calculated and measured EMFs was 40% at the rated speed frequency of 150 Hz, and the error increases in proportion to increases in the rotating frequency.

Fig. 5 shows the measured input and output powers of the prototype TFRM. The speed was increased under constant torque conditions. The input power was over four times the output power at 60 Hz. The difference between the curves (c1) and (c2) is the sum of mechanical loss and core loss [12]:

$$W_{\mathrm{in}} - (\tau\omega + W_{\mathrm{c}}) = W_{\mathrm{m}} + W_{\mathrm{i}} \tag{1}$$

where W_{in} is the input power of the motor, τ is the torque, ω is the rotational speed, W_{c} is the copper loss and W_{m} is

Fig. 2. (Color online) Fabricated stator outer core. (a) Core without slits, (b) Core with slits.
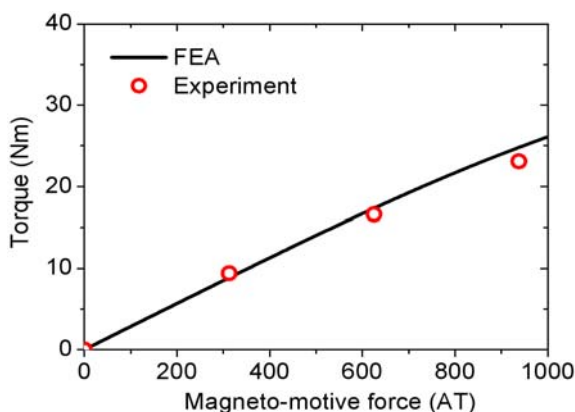

Fig. 3. (Color online) Calculated and measured static torque of the prototype TFRM.
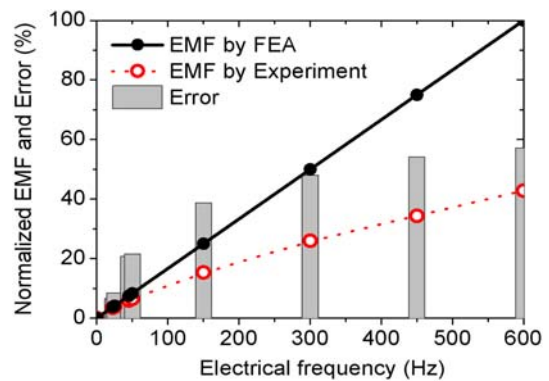

Fig. 4. (Color online) Calculated and measured no-load EMF of the prototype TFRM.
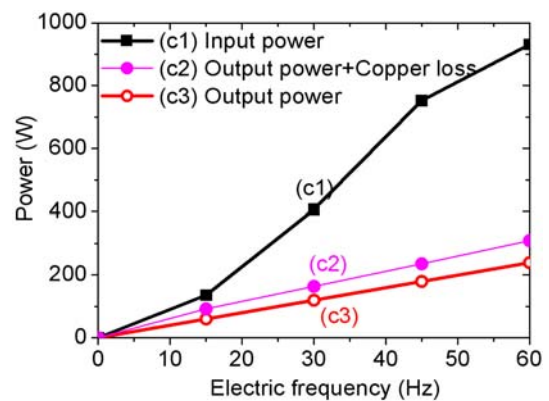

Fig. 5. (Color online) Measured powers for constant torque and variable speed.

the mechanical loss, which is the sum of the windage and friction losses. W_{i} includes the stator and rotor core losses. In general, the mechanical loss can be ignored compared to core loss because the windage loss is trivial at low speeds and friction loss is also negligible due to bearings. Therefore, it is estimated that the error in Fig. 4 and the difference between the curves (c1) and (c2) in Fig. 5 are due to core losses.

Additionally, in the previous work [13], various magnetic core combinations were examined for the stator in a TFRM. The results showed that stator core loss was a big portion of total core loss and the core loss was the most severe when the stator has ring shaped outer core sheets as shown in Fig. 1(b).

4. Slit Effects

4.1. Experimental approach

In section III, it was shown how serious the core loss problem is in prototype TFRM. In order to find a solution, an experimental approach was considered first. The

process to derive the idea for this experimental approach was as follows:

1) The stator cores of general LFRMs are also ring shaped, but the magnetic flux path is totally different from TFRMs. In the case of LFRMs the number of magnetic polarities along the circumference is equal to the number of rotor poles, so they have several magnetic flux paths in the stator core.

2) In the case of the TFRM, however, the number of magnetic polarities along the circumference is only one. For example, if current flows counter-clockwise, the polarities of the upper outer core are all N and the polarities of the lower outer core are all S. The flux path is only one way from the lower core to the upper core. This causes an eddy current to flow along the the circumference of the stator outer core leading to large eddy current losses.

3) In order to reduce these eddy current losses, the length of the eddy current flow should be shortened. Therefore, slits are adopted as shown in Fig. 2(b).

We wished to ascertain experimentally the effect of the slits so that EMFs are measured according to increasing frequency and number of slits in the outer core of the stator in the prototype TFRM. The mechanical support frame becomes weak as the number of slits is increased by adding them to the stator after finishing each test instead of making several stators for each slit model. Therefore, transformer EMF is measured, by changing winding current frequency, rather than motional EMF, measured by rotation of the rotor.

Fig. 6 shows the results of the EMF tests as a function of electric frequency under no load conditions. As mentioned before, sinusoidal currents were excited in one of the parallel circuits in the stationary state of the rotor, and the EMFs were measured in the other circuit. The EMF values were normalized on the basis of the EMF when the electric frequency is 600 Hz and the number of slit, Ns, is
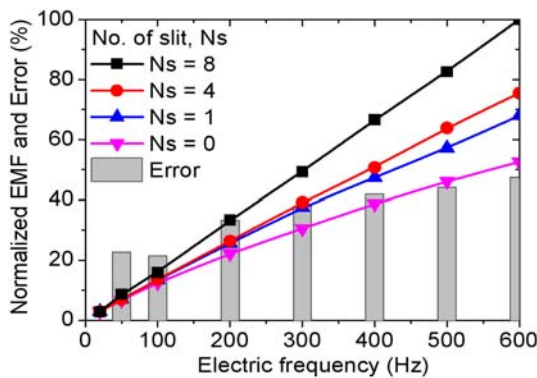
8. When the stator core has no slit (Ns = 0), the curve of the EMF is highly non-linear with respect to frequency, but as the number of the slits increases the EMF characteristics become more linear. This experimental result indicates that the core losses are reduced by increasing the number of slits.

4.2. Analysis results

In order to confirm the slit effect by numerical analysis, eddy current loss was calculated using 3D FEA. Since experimentally transformer EMFs were measured as shown in Fig. 6 and motional EMFs were measured as shown in Fig. 4, both EMFs were considered as the eddy current sources in the electromagnetic field analysis.

Fig. 7 shows the eddy current losses that occurred by each transformer and motional EMFs at speeds of 100, 200 and 300 rpm and with the number of slits increasing from 0 to 30. These eddy current losses were normalized on the basis of the maximum eddy current loss when number of slits is zero and the speed is 300 rpm. Since the source quantity is different, the losses are also different between the cases of motional and transformer EMFs. Therefore, the normalized values are compared, and the differences between the curves with solid and open symbols indicate neither difference of loss nor the difference of influence. An important point to note is that the eddy current losses by transformer and motional EMFs are similar in terms of the fact that eddy current loss is decreased as number of slits is increased. At 300 rpm, eddy current loss was reduced by 45~55% when the number of slits is 30, and the percentage of improvement is similar to the error percentage between the calculated and measured EMFs at the same speed, as shown in Fig. 4. In practice, the results for motional EMF of a new fabricated TFRM with 30 slits in the stator outer core, as shown in Fig. 2(b), perfectly agreed with the calculated EMF, and
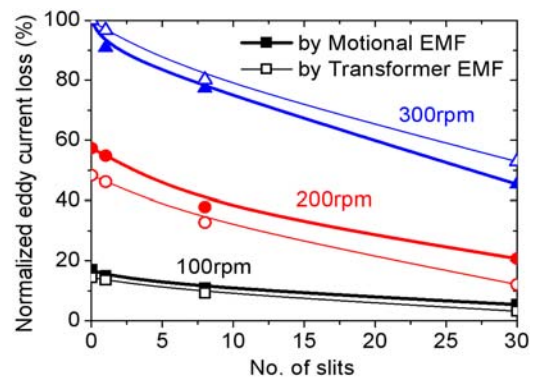

Fig. 6. (Color online) Measured EMF according to number of slits and rotor speed. (Error is the difference between the values at Ns = 0 and at Ns = 8).

Fig. 7. (Color online) Calculated eddy current losses according to number of slits, rotor speed, and source type (solid symbols are motional EMF, and open symbols are transformer EMF).
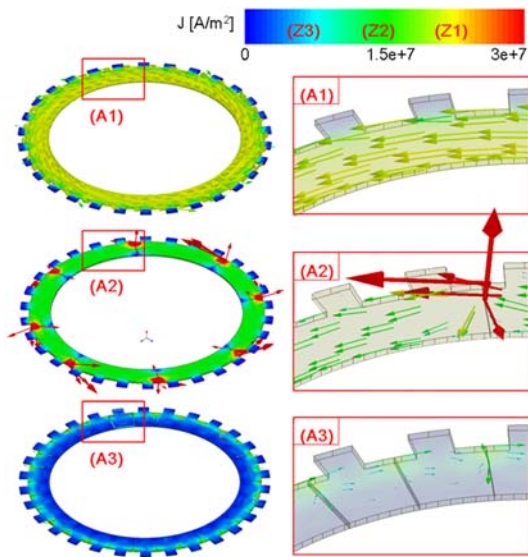
Fig. 8. (Color online) Eddy current distribution by motional EMF depending on number of slits (Ns) at 300 rpm: (A1) Ns = 0, (A2) Ns = 8, (A3) Ns = 30.

the curve is a straight line as the speed increases [13].

Fig. 8 shows the eddy current density and its vector diagrams on a stator outer core sheet against the number of slits at a speed of 300 rpm. When the number of slits is zero, the eddy current vectors move around in one big circle, and the average eddy current density at this moment is in the (z1) region in the eddy current density spectrum. If the number of slits is 8 or 30, the eddy current path is discontinuous and the average current densities are reduced into the (z2) and (z3) regions of the spectrum, respectively. The distribution of the loss over the core sheets with slits is non-uniform, and most of the loss is concentrated near the edges of the slits. However, it is noticeable that when the number of slits is 30, the eddy current loss concentrated in the slits is remarkably reduced compared to when the number of slits is 8.

5. Conclusion

Experimentally and analytically it was confirmed that slits are an efficient method to reduce eddy current loss in TFRMs with ring shaped steel sheets. The core loss decreases when the number of slits is increased. When the number of slits was equal to the number of stator teeth, the curve of EMF against speed became linear. In addition, it was confirmed that the improvement percentage of the EMF is similar to reduction percentage of the calculated eddy current losses.

References

[1] B. C. Mecrow and A. G. Jack, IEEE Trans. Magn. **28**, 1122 (1992).
[2] K. Yamazaki, S. Tada, H. Mogi, Y. Mishima, C. Kaido, K. Takahashi, K. Ide, K. Hattori, and A. Nakahara, IEEE Trans. Magn. **44**, 1502 (2008).
[3] R. Lin, A. Haavisto, and A. Arkkio, IEEE Trans. Magn. **46**, 3933 (2010).
[4] Y. Gao, K. Muramatsu, K. Shida, K. Fujiwara, S. Fukuchi, and T. Takahata, IEEE Trans. Magn. **45**, 1044 (2009).
[5] S. Nogawa, M. Kuwata, D. Miyagi, T. Hayashi, H. Tounai, T. Nakau, and N. Takahashi, IEEE Trans. Magn. **41**, 2024 (2005).
[6] Y. Kamiya and T. Onuki, IEEE Trans. Magn. **32**, 741 (1996).
[7] J. Y. Lee, D. K. Hong, B. C. Woo, and J. P. Hong, Digests of the 2010 14th Biennial IEEE Conf. on Electromagnetic Field Computation, Chicago (2010).
[8] P. Zhou, Z. Badics, D. Lin, and Z. J. Cendes, IEEE Trans. Magn. **44**, 718 (2008).
[9] D. Lin, P. Zhou, and Q. M. Chen, IEEE Vehicle Power and Propulsion Conf. (VPPC), Harbin, China (2008).
[10] J. Y. Lee, S. R. Moon, D. H. Kang, and J. P. Hong, Proc. of the 17th Conf. on the Computation of Electromagnetic fields (Compumag), Florianopolis, Brazil, 608 (2009).
[11] Erich Schmidt, IEEE Trans. Magn. **41**, 836 (2005).
[12] K. Yamazaki, Y. Fukushima, and M. Sato, IEEE Trans. Ind. Appl. **45**, 1334 (2009).
[13] J. Y. Lee, S. R. Moon, D. H. Koo, D. H. Kang, G. H. Lee, and J. P. Hong, J. Electrical Engineering & Technology **6**, 350 (2011).